Available online at www.sciencedirect.com
ScienceDirect
Chinese Journal of Natural Medicines 2019, **17**(4): 0275–0290
Chinese Journal of Natural Medicines

A novel approach based on metabolomics coupled with network pharmacology to explain the effect mechanisms of Danggui Buxue Tang in anaemia

HUA Yong-Li*, MA Qi, YUAN Zi-Wen, ZHANG Xiao-Song, YAO Wan-Ling, JI Peng, HU Jun-Jie, WEI Yan-Ming

College of Veterinary Medicine, Gansu Agricultural University, Lanzhou 730070,China

Available online 20 Apr., 2019

[ABSTRACT] Danggui Buxue Tang (DBT) is a famous Chinese medicinal decoction. Mechanism of DBT action is wide ranging and unclear. Exploring new ways of treatment with DBT is useful. Sprague–Dawley(SD) rats were randomly divided into 3 groups including control (NC, Saline), the DBT (at a dose of 8.10 g·kg^{-1}), and blood deficiency (BD) (Cyclophosphamide (APH)- and Cyclophosphamide(CTX)-induced anaemia). A metabolomics approach using Liquid Chromatography-Quadrupole-Time-of-Flight/Mass Spectrometry (LC/Q-TOFMS) was developed to perform the plasma metabolic profiling analysis and differential metabolites were screened according to the multivariate statistical analysis comparing the NC and BD groups, and the hub metabolites were outliers with high scores of the centrality indices. Anaemia disease-related protein target and compound of DBT databases were constructed. The TCMSP, ChemMapper and STITCH databases were used to predict the protein targets of DBT. Using the Cytoscape 3.2.1 to establish a phytochemical component–target protein interaction network and establish a component, protein and hub metabolite protein–protein interaction (PPI) network and merging the three PPI networks basing on BisoGenet. The gene enrichment analysis was used to analyse the relationship between proteins based on the relevant genetic similarity by ClueGO. The results shown DBT effectively treated anaemia *in vivo*. 11 metabolic pathways are involved in the therapeutic effect of DBT *in vivo*; *S*-adenosyl-L-methionine, glycine, L-cysteine, arachidonic acid (AA) and phosphatidylcholine(PC) were screened as hub metabolites in APH- and CTX-induced anaemia. A total of 288 targets were identified as major candidates for anaemia progression. The gene-set enrichment analysis revealed that the targets are involved in iron ion binding, haemopoiesis, reactive oxygen species production, inflammation and apoptosis. The results also showed that these targets were associated with iron ion binding, haemopoiesis, ROS production, apoptosis, inflammation and related signalling pathways. DBT can promote iron ion binding and haemopoiesis activities, restrain inflammation, production of reactive oxygen, block apoptosis, and contribute significantly to the DBT treat anaemia.

[KEY WORDS] Danggui Buxue Tang; Metabolomics; Network pharmacology; Anaemia

[CLC Number] R965 **[Document code]** A **[Article ID]** 2095-6975(2019)04-0275-16

Introduction

Danggui Buxue Tang (DBT) is a famous Chinese medicinal decoction which is composed of *Astragalus membranaceus* (Fisch.) Bunge(Huangqi, AR) and *Angelicae Sinensis* Radix (Danggui, AS) at the ratio of 5 : 1 (*W*/*W*) used for treating blood deficiency (BD) in traditional Chinese medicine (TCM) and was first recorded in by Li Dongyuan in China [1]. According to the references, the DBT can treat BD and some type of anaemia [2]. BD is a state of systemic weakness caused by bleeding and weakness of organs. It leads to disturbance of substance and blood, dizziness, numbness of limbs, pallor, insomnia, palpitation, weak pulse and so on. BD is also a common syndrome in the clinical practice of TCM [3-4]. The syndrome is caused by spleen disorders, blood loss and blood diseases [5-6]. Moreover, the increasing pace of life contributes to these disorders. DBT had an obvious treat effect on immune-mediated aplasia anaemia models mice [1] and Blood

[Received on] 11-Dec.-2018

[Research funding] This work was supported by the National Natural Science Foundation of China (Nos. 31560709 and 31472234) and the College of Veterinary Medicine of Gansu Agricultural University (No. JYCX-KX005).

[*Corresponding author] Tel: 86-931-7631229; E-mail: huayongli2004@163.com.

These authors have no conflict of interest to declare.

loss anaemia [7]. DBT also can stimulates the transcript expression of oestrogen-responsive genes [8]. DBT exerts good therapeutic effects on hepatic fibrosis [9]. Pharmacological results showed that DBT promotes the proliferation and differentiation of bone cells [10]. Hence, the therapeutic effect of DBT is achieved through their active ingredient complex with multiple targets and paths in the human body. However, these active components cannot be accurately detected using routine methods [11-12]. In spite of a lot of study to look for the therapeutic mechanism of DBT, combination of multiple components of DBT work together to produce its clinical effect is unclear. Conventional pharmacological approaches cannot understand the systems-level mechanism of DBT. Therefore, new methods which can used to study the systems-level mechanism are needed.

Network pharmacology is a new subject that selects specific signal nodes for multitarget drug molecule design through multitarget network analysis of biological systems [13]. Recently, network pharmacology can proclaim the mechanisms of TCM medicines at the systems level [14]. The action mechanisms of some herbal formulas [15-16] were clarified based on the Network pharmacology. For examples, the active ingredients and potential targets of Yangxinshi tablet were predicted based on network pharmacology strategy for treating heart failure [17], the molecular mechanisms of Ban-Xia-Xie-Xin-Tang were uncovered by network Pharmacology Approach [15], Tongmai Yangxin pills anti-oxidative stress alleviates cisplatin-induced T cardiotoxicity network pharmacology analysis and experimental evidence [18], and so on. Moreover, the network pharmacology integrated with molecular mechanism and metabolomics strategy was used in TCM research, anti-inflammatory effects of Zhishi and Zhiqiao revealed [19], the material basis and the mechanism for anti-renal interstitial fibrosis efficacy of Rhubarb [20], and so on. All the references proved the network pharmacology integrated with metabolomics strategy was effective method and can be used to study the effect and mechanism of TCM.

Therefore, we adopted a comprehensive method to determine the active compounds of DBT by using drug parameters and identify many medicine targets through network analysis based on existing databases and metabolomics. This method has been used to elucidate the mechanisms and synergies of multicomponent and multi-objective drugs, including other TCM formulations [21]. As our understanding improves so do we recognised more clearly the need for the systems (poly)pharmacology [22].

Materials and Methods

Our scheme consisted of six main steps: (1) Pharmacological test; (2) Metabolomics screening and pathway enrichment analysis of biomarkers and constructing an extended metabolic pathway protein that interacts with the network; (3) Screening of target proteins for DBT and establishing a phytochemical component–target protein interaction network; (4) Identification of active ingredients that are absorbed into the blood and constructing interaction networks of absorbed components and target protein; (5) Establishing a component, protein and metabolite protein–protein interaction (PPI) network and merging the three PPI networks; (6) Explaining the hub targets and elucidating the mechanisms of the therapeutic effects of DBT on anaemia. The entire frame is shown in Fig. 1.

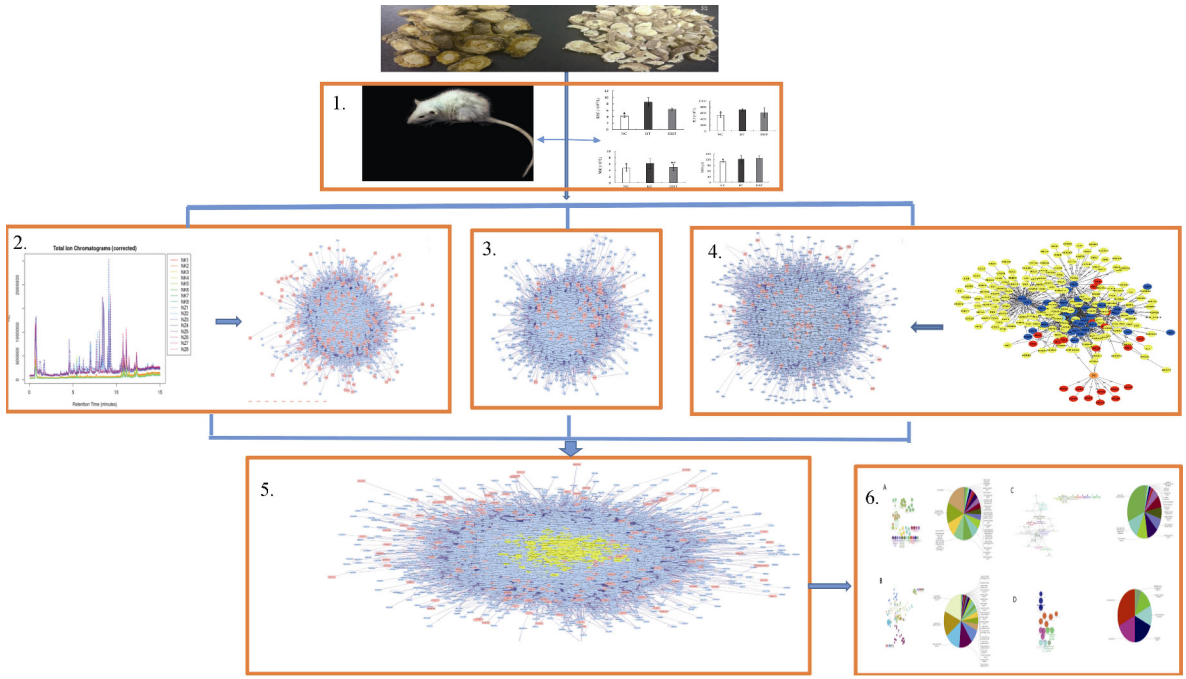

Fig. 1 Process overview. 1. Pharmacological test; 2. Metabolomics study of plasma; 3. Anemia-related targets network; 4. Compound-putative targets network; 5. Merged the three networks; 6. Enrichment analysis of candidate targets

Materials

AS and AR were purchased from Tianyuan Medicinal materials company (Lanzhou, China). AR come from the root of *Astragalus membranaceus* (Fisch.) Bge. (voucher no: AR-20170616). AS come from the root of *Angelica sinensis* (Oliv.) Diels (Umbelliferae) and processing with wine (voucher no: AS-20170616). AS and AR had been identified by Prof. WEI Yan-Ming (Gansu Agricultural University, Lanzhou, China), were deposited at herbarium center of Gansu Agriculture University. HPLC grade acetonitrile and methanol and were purchased Fisher Scientific (Waltham, MA, USA).

Preparation of samples

DBT was extracted from AR (500 g) and AS (100 g). The mixture (AR and AS) were boiled twice (90 min and 45 min, respectively), and two decoctions were merged, filtering, enrichment and freeze-dried. The last, the drug powder (250 g) was storage at 4 °C.

Mainly components analysis in DBT

To standardize DBT chemically, formononetin and calycosin are main components in AR, ferulic acid is main component in the AS, were selected as marker chemicals [23]. DBT drug powders were weighted, dissolved in ultrapure water level 1 mL of liquid to 1 g original medical material analysis measurement.1 mL of DBT was diluted into 100 mL methanol, and concentrating with 20 minutes, 10 minutes in 12 000 r·min^{-1} and filtering 0.45 μm membranes. Agilent 1260 separate module system with Agilent Zorbax XDB-C_{18} column (5 μm, 25 mm × 4.6 mm) was by used to analyze the formononetin, calycosin and ferulic acid.

Metabolomic profiling

Herb administration and animals

Sprague–Dawley (SD) rats (200–220 g) were purchased from the Experimental Animal Center of Gansu Province (Gansu, China). After one week, the rats (sex in half), according to the principle of randomized, were separated into control (NC, 8 rats), model (BD, 8 rats) and DBT (8 rats) group. The rats in the BD and DBT groups were hypodermically injected with 2% acetylphenylhydrazine (APH) saline solution on days 1 and 4 at dose of 20 and 10 mg·kg^{-1}, respectively. Two hours after the hypodermic injection with 2% APH saline solution on day 4, the rats were intraperitoneally injected with cyclophosphamide (CTX) saline solution on days 4, 5, 6 and 7 at a dose of 20 mg·kg^{-1} [4, 24] to reproduce the BD model. The rats in the DBT group were administered with DBT extracts intragastrically at a dose of 8.10 g·kg^{-1} (8.10 g crude herbs per 1 kg rat body weight) dissolved and dispersed homogeneously in ultrapure water. The animal dose of DBT extracts was extrapolated from the human daily dose by using the body surface area normalisation method. The formula for the dose translation was as follows: human dose of crude herbs in clinic × 0.018/200 × 1000 × the multiple of clinical equivalency dose. The dose of the DBT extracts was equivalent to that of crude herbs based on the TCM prescription. The NC and BD groups were given the same volume of saline solution. Animals in DBT group were administration by gavage once one day for 10 consecutive days.

The protocol was authorized by the Animal Experimental Ethical Committee of Gansu Agricultural University. Every effort was made to alleviate animal suffering.

Sample collection

Blood samples (0.7 mL) from the rats were gathered using the posterior orbital venous plexus approach.

Index analysis and peripheral haemogram assay

The blood was sampled from the posterior orbital venous plexus for the routine blood assay, including red blood cells (RBC), white blood cells (WBC), platelets (PLT), haematocrit and haemoglobin (HGB), by using the Sysmex F-820 semi-automatic blood analyser (East Asia Company, Japan).

Metabolomic profiling

Plasma samples were diluted with acetonitrile (*V*/*V*, 50 : 200 μL) for protein removal. Each sample contained *N*-formylanthranilic acid and lysoPC (19 : 0) as internal standards at an ultimate concentration of 30 and 1.875 ng·μL^{-1}, respectively. Unbiased metabolic profiling was performed using Liquid Chromatography coupled to quadrupole–time-of-flight mass spectrometry (LC/Q-TOFMS) on an Agilent 1290 Infinity LC system Zorbax SB-C_{18} column (2.1 mm × 100 mm, 1.8 μm) and Agilent 6530 LC/Q-TOFMS (Agilent Technologies, Inc., Santa Clara, CA) operated in positive electrospray ionisation and negative electrospray ionisation modes. The table 1 was shown the mobile phase which consisted of 0.1% aqueous formic acid (*V*/*V*) (A) and acetonitrile that contained 0.1% formic acid (*V*/*V*) (B). Leucine enkephalin was used as the reference mass. A quality control (QC) sample was used to ensure system stability and repeatability. Positive and Negative ion mode for testing the mass spectrum of conditions were shown in Table 2.

Table 1 The gradient of mobile phase

t/min	Flow (mL·min^{-1})	Injection volume of the samples (μL)	Pressure limit (bar)	Solv ratio A (%)
0	0.35	4	800	3
1	0.35	4	800	3
8	0.35	4	800	70
10	0.35	4	800	70
17	0.35	4	800	90
18	0.35	4	800	100
21	0.35	4	800	100
26	0.35	4	800	3

Table 2 The parameter and for testing the mass spectrum of conditions

Item	Positive ion mode	Negative ion mode
capillary voltage	4 kV	3.5 kV
Sampling cone	35 kV	50 kV
Source temperature	100 °C	100 °C
Desolvation temperature	350 °C	300 °C
Cone gas flow	50 $L \cdot h^{-1}$	50 $L \cdot h^{-1}$
Desolvation gas flow	600 $L \cdot h^{-1}$	700 $L \cdot h^{-1}$
Extraction cone	4 V	4 V
Scan time	0.03 s	0.03 s
Interscan time	0.02 s	0.02 s
range of data collection	50–1000 *m/z*	50–1000 *m/z*

Metabolomic data preprocessing

The based LC/Q/TOF-MS metabolomic profiling data were imported into a MassHunter Qualitative Analysis workstation to execute the metabolic feature extraction by adopting a molecular feature extraction algorithm (Agilent Technologies, Inc., Santa Clara, CA). The resultant metabolic features were submitted to GeneSpring MS 1.2 (Agilent Technologies, Inc., Santa Clara, CA) for chromatographic and mass spectrometric alignment and sequentially handled using the XCMS software running under R environment version 2.3.1 for metabolic feature detection and chromatographic matching [25] (Fig. 2).

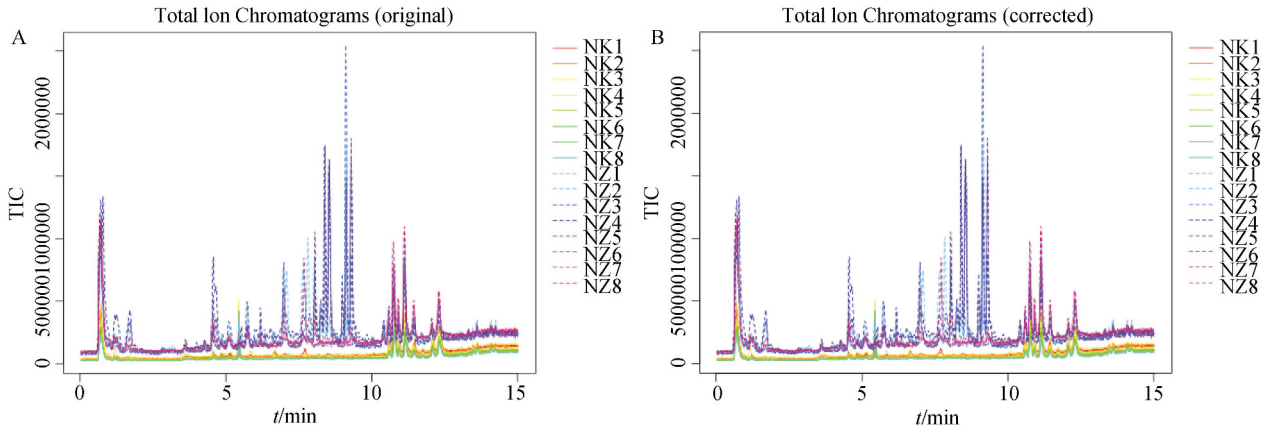

Fig. 2 The total ion current (TIC) profiles by using LC-Q/TOF-MS. (A) Original TIC. (B) Corrected TIC by using the XCMS software

Dataset trimming and normalisation

For the LC/Q-TOFMS-based metabolomic data, the noise of the metabolic dataset signals was first filtered with 10 000 as the threshold. The data was further filtered using the '80% rule'. The metabolic feature measurements were normalized to internal standards. Prior to multivariate analysis, the LC/Q-TOFMS-based data were first mean-centred and then scaled to the square root of standard deviation. A total of 2268 metabolite signals (1263 from the positive ion mode and 1005 from the negative ion mode) from all plasma were detected after the metabolic peak detection and alignment. After data reduction, standardization and trimming by using the '80% rule' to reduce the missing value input, 510 metabolite signals from LC/Q-TOFMS remained in the ultimate metabolite dataset for further analysis.

Biomarker screening and chemical elucidation of significant characteristics

The differential metabolites or metabolic features of the BD, NC and DBT groups were screened using the S-plot of the principal component analysis (PCA) and orthogonal projection to latent structures–discriminant analysis (OPLS-DA) models. The adjusted *P*-value of the inter-group nonparametric test (Mann–Whitney U test) for the potential differential metabolites was less than 0.05. For the metabolite structure elucidation in LC/Q-TOFMS analysis, a previously reported identification strategy was employed and mainly included searching online databases with exact *m/z* values (HMDB: http: //www.hmdb.ca/; METLIN: http: //metlin.scripps.edu/; KEGG: http: //www.kegg.com/; and LIPID MAPS: http: //www.lipidmaps.org/), comparing the acquired MS/MS spectra with standard records (HMDB; METLIN; and MassBank: http: //www.massbank.jp/) and MS/MS spectra interpretation and validation with available standard compounds.

Pathway enrichment analysis of biomarkers and enrichment network construction

MetaboAnalyst 2.0, a comprehensive tool suite for metabolomic data analysis, was used to enrich the pathway of

biomarkers. The metabolites derived from the enrichment pathways were extended to their nearest neighbours. The hub metabolites were outliers with high scores of the centrality indices using Cytoscape 3.2.1. According to the references [26], We uses two well-established node centrality measures to estimate node importance – degree and betweenness centrality. To select hub metabolites in the current network, these differential metabolites were validated using an independent sample degree (> 10) and BetweennessCentrality (> 0.1). The new hub metabolite–pathway protein interaction (PPI) network was constructed using BisoGenet [27].

Chemical composition of DBT

The composition of the two herbaceous plant species of DBT was obtained from the TCM Systems Pharmacology Database (http: //tcmspnw.com/, version: 2.0, TCMSP) and chemistry database of the Chinese Academy of Sciences (http: //www.organchem.csdb.cn/, last updated: October 18, 2017) [28]. A total of 55 kinds of chemical substances were found (Table 4), including 39 kinds from AS and 16 from AR [29]. We manually searched reports of these candidate compounds for further analysis. By using the calculation results of Wang and others [30], we estimated the oral bioavailability (OB) of the oral dose in the bloodstream [31] and the drug likeness (DL) between the clinical drug and the drug in the blood. Drug compounds with 30% OB and 0.18 DL were selected as candidate drug compounds.

Table 3 Effect of the DBT decoction on the peripheral haemogram of anaemia rats

Group	RBC/×10^{12}/L	WBC/×10^{9}/L	HGB/g·L^{-1}	PLT/×10^{9}/L
NC	8.51 ± 1.39	6.15 ± 1.65	122.7 ± 18.19	707.1 ± 36.17
BD	4.17 ± 0.37▲	4.64 ± 0.94▲	110.0 ± 6.16▲	523.4 ± 66.04▲
DBT	6.33 ± 0.28	4.92 ± 1.02□▲	128.6 ± 3.36□	613.3 ± 160.37

Note: ▲$P < 0.05$ *vs* NC group; □$P < 0.05$ *vs* BD group

Table 4 Bioactive compounds with their predicted OB and DL values

ID	Compound name	OB	DL	Herbs
DG01	*α*-Spinasterol	42.98	0.76	Radix Angelicae Sinensis
DG02	Marmesinin	82.28	0.18	Radix Angelicae Sinensis
DG03	*Z*-Ligustilide	48.44	0.07	Radix Angelicae Sinensis
DG04	Archangelicin	37.1	0.65	Radix Angelicae Sinensis
DG05	Flazine	109.3	0.39	Radix Angelicae Sinensis
DG06	Columbianedin	87.14	0.36	Radix Angelicae Sinensis
DG07	Angelol B	67.86	0.35	Radix Angelicae Sinensis
DG08	Oxypeucedanin hydrate	36.01	0.29	Radix Angelicae Sinensis
DG9	Columbianetin acetate	52.06	0.26	Radix Angelicae Sinensis
DG10	2″-*O*-(2‴-Methylbutyryl)-isoswertisin_qt	33.78	0.24	Radix Angelicae Sinensis
DG11	Isoimperaterin	39.38	0.24	Radix Angelicae Sinensis
DG12	Imperatorin	31.01	0.23	Radix Angelicae Sinensis
DG13	Berfeldine	42.11	0.18	Radix Angelicae Sinensis
DG14	Nodakenin_qt	79.04	0.18	Radix Angelicae Sinensis
HQ1	Mairin	55.38	0.78	Radix Astragali seu Hedysari
HQ2	Jaranol	50.83	0.29	Radix Astragali seu Hedysari
HQ3	Hederagenin	36.91	0.75	Radix Astragali seu Hedysari
HQ4	(3*S*, 8*S*, 9*S*, 10*R*, 13*R*, 14*S*, 17*R*)-10, 13-Dimethyl-17-[(2*R*, 5*S*)-5-propan-2-yloctan-2-yl]-2, 3, 4, 7, 8, 9, 11, 12, 14, 15, 16, 17-dodecahydro-1H-cyclopenta[a]phenanthren-3-ol	36.23	0.78	Radix Astragali seu Hedysari
HQ5	Isorhamnetin	49.6	0.31	Radix Astragali seu Hedysari
HQ6	3, 9-Di-*O*-methylnissolin	53.74	0.48	Radix Astragali seu Hedysari
HQ7	5′-Hydroxyiso-muronulatol-2′, 5′-di-*O*-glucoside	41.72	0.69	Radix Astragali seu Hedysari
HQ8	7-*O*-Methylisomucronulatol	74.69	0.3	Radix Astragali seu Hedysari
HQ9	9, 10-Dimethoxypterocarpan-3-*O*-*β*-D-glucoside	36.74	0.92	Radix Astragali seu Hedysari
HQ10	(6a*R*, 11a*R*)-9, 10-Dimethoxy-6a, 11a-dihydro-6H-benzofurano[3, 2-c]chromen-3-ol	64.26	0.42	Radix Astragali seu Hedysari

Continued

ID	Compound name	OB	DL	Herbs
HQ11	Bifendate	31.1	0.67	Radix Astragali seu Hedysari
HQ12	Formononetin	69.67	0.21	Radix Astragali seu Hedysari
HQ13	Isoflavanone	109.99	0.3	Radix Astragali seu Hedysari
HQ14	Calycosin	47.75	0.24	Radix Astragali seu Hedysari
HQ15	Kaempferol	41.88	0.24	Radix Astragali seu Hedysari
HQ16	FA	68.96	0.71	Radix Astragali seu Hedysari
HQ17	(3*R*)-3-(2-Hydroxy-3, 4-dimethoxyphenyl)chroman-7-ol	67.67	0.26	Radix Astragali seu Hedysari
HQ18	Isomucronulatol-7, 2'-di-*O*-glucosiole	49.28	0.62	Radix Astragali seu Hedysari
HQ19	1, 7-Dihydroxy-3, 9-dimethoxy pterocarpene	39.05	0.48	Radix Astragali seu Hedysari
HQ20	Quercetin	46.43	0.28	Radix Astragali seu Hedysari
HQ21	Mairin	55.38	0.78	Radix Astragali seu Hedysari
HQ22	Jaranol	50.83	0.29	Radix Astragali seu Hedysari
HQ23	Hederagenin	36.91	0.75	Radix Astragali seu Hedysari
HQ24	(3*S*, 8*S*, 9*S*, 10*R*, 13*R*, 14*S*, 17*R*)-10, 13-Dimethyl-17-[(2*R*, 5*S*)-5-propan-2-yloctan-2-yl]-2, 3, 4, 7, 8, 9, 11, 12, 14, 15, 16, 17-dodecahydro-1*H*-cyclopenta[a]phenanthren-3-ol	36.23	0.78	Radix Astragali seu Hedysari
HQ25	Isorhamnetin	49.6	0.31	Radix Astragali seu Hedysari
HQ26	3, 9-Di-*O*-methylnissolin	53.74	0.48	Radix Astragali seu Hedysari
HQ27	5′-Hydroxyiso-muronulatol-2′, 5′-di-*O*-glucoside	41.72	0.69	Radix Astragali seu Hedysari
HQ28	7-*O*-Methylisomucronulatol	74.69	0.3	Radix Astragali seu Hedysari
HQ29	9, 10-Dimethoxypterocarpan-3-*O*-*β*-D-glucoside	36.74	0.92	Radix Astragali seu Hedysari
HQ30	(6aR, 11aR)-9, 10-Dimethoxy-6a, 11a-dihydro-6*H*-benzofurano[3, 2-c]chromen-3-ol	64.26	0.42	Radix Astragali seu Hedysari
HQ31	Bifendate	31.1	0.67	Radix Astragali seu Hedysari
HQ32	Formononetin	69.67	0.21	Radix Astragali seu Hedysari
HQ33	Isoflavanone	109.99	0.3	Radix Astragali seu Hedysari
HQ34	Calycosin	47.75	0.24	Radix Astragali seu Hedysari
HQ35	FA	68.96	0.71	Radix Astragali seu Hedysari
HQ36	(3*R*)-3-(2-Hydroxy-3, 4-dimethoxyphenyl) chroman-7-ol	67.67	0.26	Radix Astragali seu Hedysari
HQ37	Isomucronulatol-7, 2'-di-*O*-glucosiole	49.28	0.62	Radix Astragali seu Hedysari
HQ38	1, 7-Dihydroxy-3, 9-dimethoxy pterocarpene	39.05	0.48	Radix Astragali seu Hedysari
HQ39	Quercetin	46.43	0.28	Radix Astragali seu Hedysari

Target selecting of candidate compounds in DBT and network construction

The protein targets of the bioactive compounds were predicted by using the TCMSP, ChemMapper, STITCH databases. Then, the compound−target (C-T) networks and their fundamental topological properties were constructed using Cytoscape 3.2.1.

Identifying anaemia-related targets

The anaemia-related targets were identified using three kinds of existing resources. In (1) DrugBank, we searched FDA-approved drugs to treat anaemia, studied the interaction between human gene and protease targets and acquired 14 anaemia-related targets [32]. In the (2) Online Mendelian Inheritance in Man database (http: //www.omim. org/), we used the keyword ‘anaemia’ and found 19 known anaemia-related targets [33]. In the (3) Genetic Association Database (http: //geneticassociationdb. nih.gov/), we used the keyword ‘anaemia’ and found 51 known anaemia-related targets [34]. The details of these known therapeutic targets are described in Supplemental Table S5. Redundancies were discarded, and a total of 84 kinds of known anaemia-related targets were collected. PPI data was obtained using the Cytoscape plug-in BisoGenet. Six existing PPI databases were analysed. These databases included IntAct, a human protein reference database, a molecular interaction database, an interactive protein database, an interactive data collection of biological compound database and a biomolecular interaction network library database [27].

Network structure of anaemia-related targets, the predicted DBT drug targets

The hub metabolite–pathway protein interaction (PPI) network, known anaemia-related target PPI network and pre-

dicted DBT drug targets protein interaction (PPI) network were constructed and merged the three PPI networks according to the obtained cell surface data from BisoGenet [35]. The topological properties of each node in the interaction network were evaluated by calculating the six indexes, namely, 'betweenness centrality (BC)', 'degree centrality (DC)', 'closeness centrality (CC)', 'network centrality (NC)', 'eigenvector centrality (EC)' and 'local average connectivity (LAC)'. These were the definitions and formulas of the defined parameters; they represented the topology of nodes in the network [36]. A high value indicated the importance of the node in the network.

Genetic ontology and path strengthening analysis

We used ClueGO for the enrichment of analysis of 288 candidate targets. ClueGO is a cell surface plug-in that can be used for group network visualisation of a large number of genes to avoid redundancy in biological terms [37]. The final candidates were divided into four categories: molecular function, biological process, cell component and immune system process. The ClueGO network was created using kappa statistics, which reflected the relationship between terms based on the relevant genetic similarity.

RESULTS

Quality evaluation of DBT

Fig. 3A and Fig. 3B showed HPLC chromatogram of reference compounds including calycosin, formononetin and ferulic acid and the HPLC chromatogram of DBT, and the peaks of calycosin, formononetin and ferulic acid were pointed out. After calculation, the content of calycosin, formononetin and ferulic acid in DBT was 0.67, 0.83 and 1.19 mg·g^{-1} respectively.

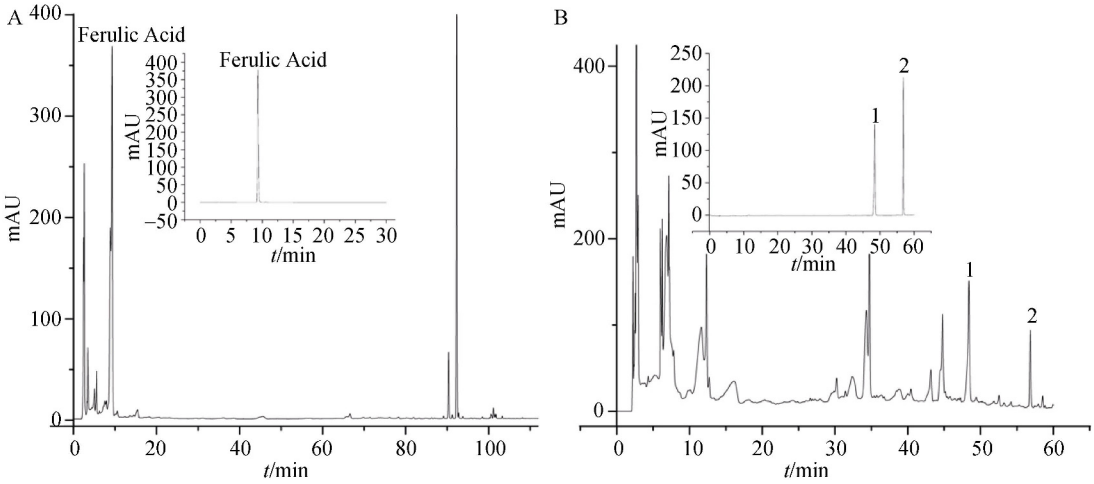

Fig. 3 HPLC chromatogram of ferulic acid, calycosin and formononetin in DBT. A. HPLC chromatogram of ferulic acid in DBT. B. HPLC chromatogram of calycosin and formononetin. The analytes of ferulic acid were separated by isocratic elution with the mobile phase of fermononetin and 0.085% phosphoric acid (17 : 83) at a flow rate of 0.8 mL·min^{-1}; UV detection: 316 nm. The method of calycosin and fermononetin: water (A) and acetonitrile (B) using a gradient program of 5% (B) in 0–10 min, 5%–10% (B) in 10–20 min, 10%–23.5% (B) in 20–40 min; 23.5%–34.5% (B) in 50–60 min; 34.5%–55% (B) in 60–70min; flow rate: 1 mL·min^{-1}; UV detection: 260nm. (1) calycosin; (2) formononetin

Pharmacological test

Behaviour of BD rats

Rats with BD appeared exhausted. They exhibited sluggish movements and sallow complexion. Their bodies curled into a ball with raised hairs. They were asthmatic and somnolent. Their tail, face, ears and eyes were pale and cool. All of these signs matched those of BD. DBT can obviously improve these symptoms.

Influence of DBT on routine blood assay results of BD rats

Table 3 shown the results of Blood routine in the BD, NC and DBT group. The RBC, PLT and HGB were decreased significantly ($P < 0.05$) in the BD groups compare with the NC group. This decrease suggested that the model was successfully set up. The RBC, HGB and PLT in the DBT group were increase compared with those in BD. This result suggested that DBT improved the BD state.

Metabolomic study of plasma

Differential metabolite analysis in the NC, BD and DBT groups

The metabolite profiles of the plasma samples were performed to determine the relative levels of the metabolites in of the NC, BD and DBT groups based on LC-Q/TOF-MS analyses (Fig. 4). We selected 177 metabolites (88 from the positive model and 89 from the negative model) which had shown difference levels between the NC and BD sample groups (Wilcoxon rank–sum test: $P < 0.05$; Table S7 for the positive mode; Table S8 for the negative mode). PCA and OPLS-DA showed clear differences in the plasma metabolome among the NC, BD and DBT groups. These data points were clustered into three distinct groups in the plot map, evidently separating the NC, BD and DBT samples (Figs. 5 and 6). In general, several metabolites displayed considerable differences in the NC, BD and DBT plasma.

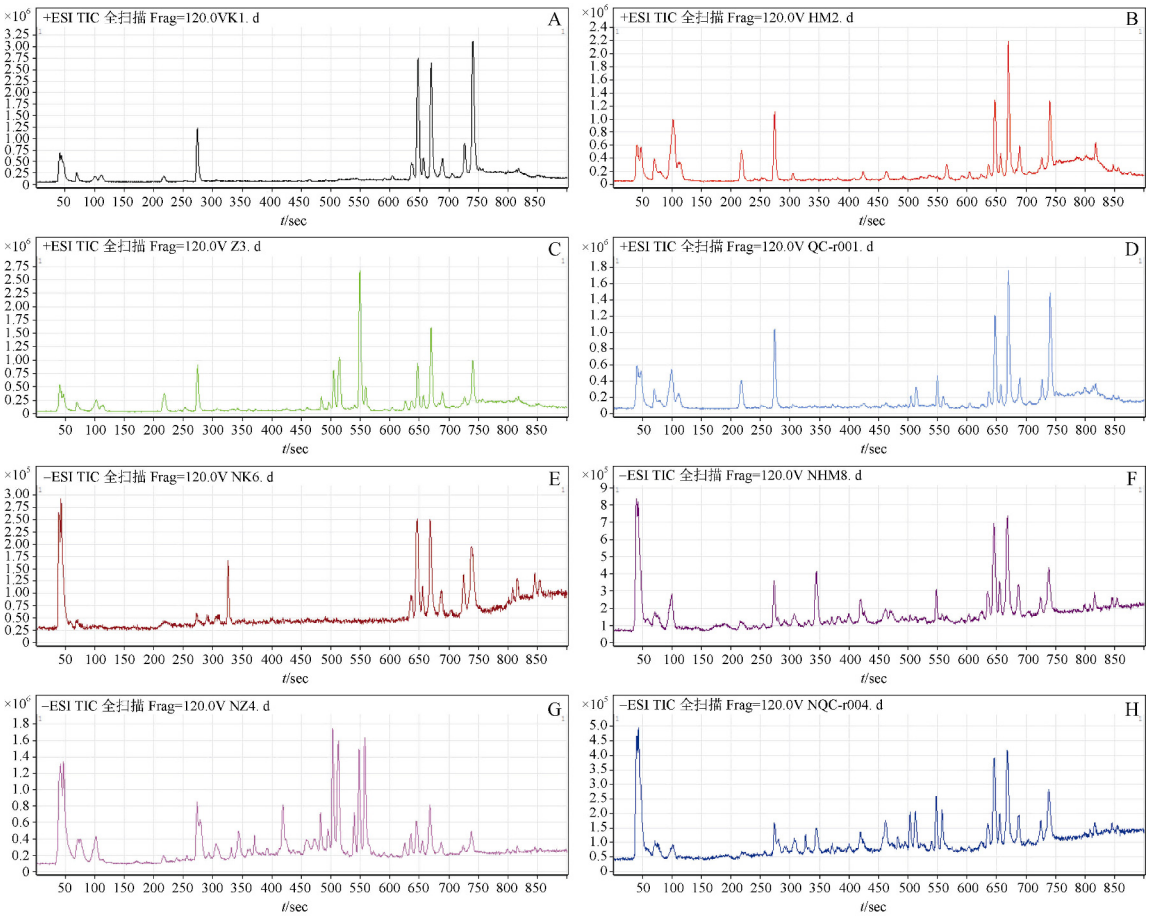

Fig. 4 Total ion chromatograms (TICs) of rat plasma samples in the positive and negative ion modes. Comparison of A (NC), B (BD), C (DBT) and D (QC) in the positive ion mode and E (NC), F (BD), G (DBT) and H (QC) in the negative ion mode

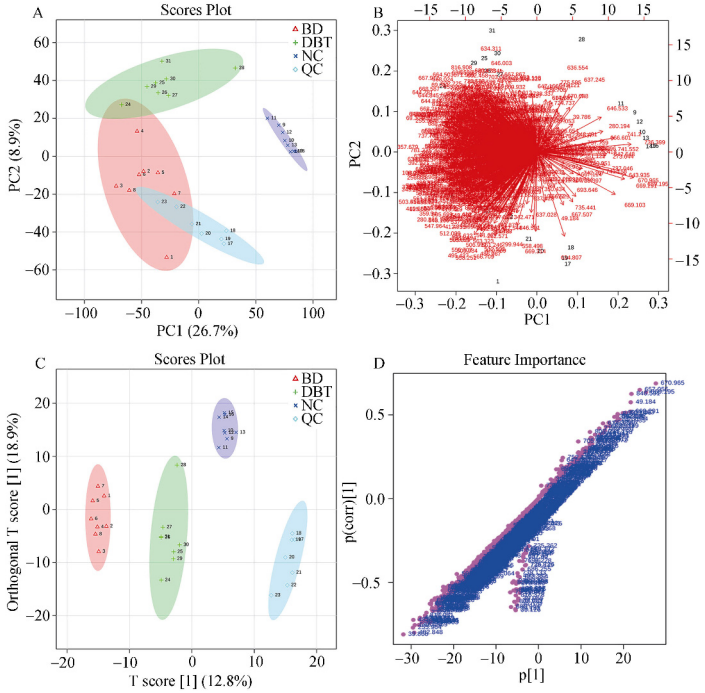

Fig. 5 PCA and OPLS-DA score plots by using LC-Q/TOF-MS in the negative ion modes. (A) PCA score plot. (B) Loading matrix graph; each point represents one variable. (C) OPLS-DA score plot. (D) Feature importance

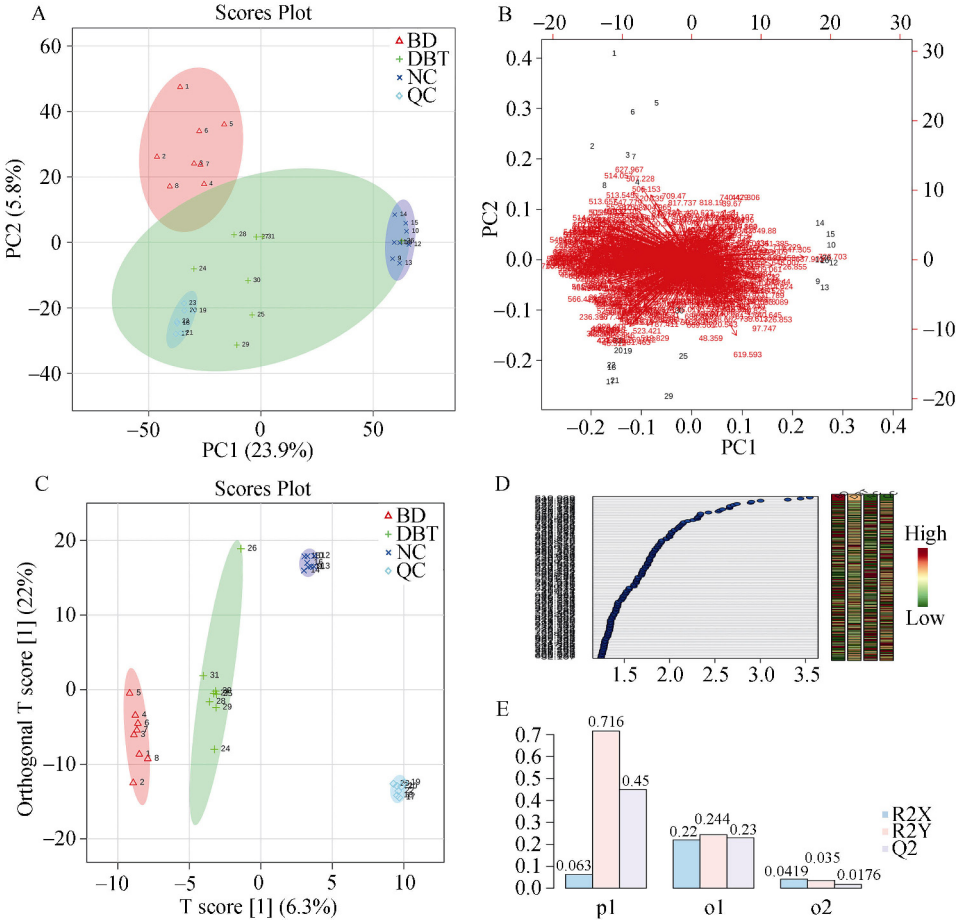

Fig. 6 PCA and OPLS-DA score plots by using LC-Q/TOF-MS in the positive ion modes. (A) PCA score plot. (B) Loading matrix graph; each point represents one variable base on the PCA. (C) OPLS-DA score plot. (D) Metabolite VIP score base on OPLS-DA. (E) Model parameters of OPLS-DA

Metabolic pathway analysis

The identified biomarkers involved in 11 pathways that were disturbed in the DBT group based on metabolic pathway analysis with MetPA (www.metaboanalyst.ca). The impact values of (a) taurine and hypotaurine metabolism; (b) alpha-linolenic acid metabolism; (c) linoleic acid metabolism; (d) glutathione metabolism; (e) arachidonic acid (AA) metabolism; (f) thiamine metabolism; (g) phenylalanine, tyrosine and tryptophan biosyntheses; (h) glycine, serine and threonine metabolism; (i) valine, leucine and isoleucine biosyntheses; (j) cysteine and methionine metabolism; and (k) arginine and proline metabolism were 0.43, 1, 1, 0.38, 0.42, 0.40, 0.5, 0.32, 0.29, 0.33 and 0.25, respectively, and were the key metabolites in each pathway (Fig. 7). The pathways with an impact value of more than 0.2 calculated from the pathway topology analysis was filtered out as the potential target pathways.

Selecting the hub metabolites of the correlation network in DBT on BD

On the basis of the metabolic pathway analysis, we selected the key metabolites that exhibited impact on 11 pathways (in red in Fig.7) The key metabolites including the list of KEGG IDs, fold change and P-values adjusted for multiple comparisons were loaded into MetScape. A metabolite–reaction–enzyme–gene graph was established to obtain an overview of all DBT metabolites on BD (Fig. 7). *S*-Adenosyl-L-methionine, glycine, L-cysteine, AA and phosphatidylcholine (PC) were selected as the hub metabolites of the correlation network in DBT on BD according to the degree (Fig. 7). Finally, we selected the genes that showed direct relationship with the hub metabolites.

Potential pharmacological mechanisms of DBT

Screening candidate compounds for DBT

The active compounds were selected and identified according the value of DL and OB in DBT known compounds [28]. 53 potential compounds have appropriate values for DL and OB from the AR and AS constituents of DBT (Table 4). The two different herbs, AR and AS contributed 39 and 14 candidate compounds, respectively.

Generating a compound–putative target network for DBT

In general, therapeutic effects of TCM on diseases rely on the synergistic effects between multiple compounds and their targets [38]. Therefore, the therapeutic targets of the predicted active compounds of DBT were explored from existing

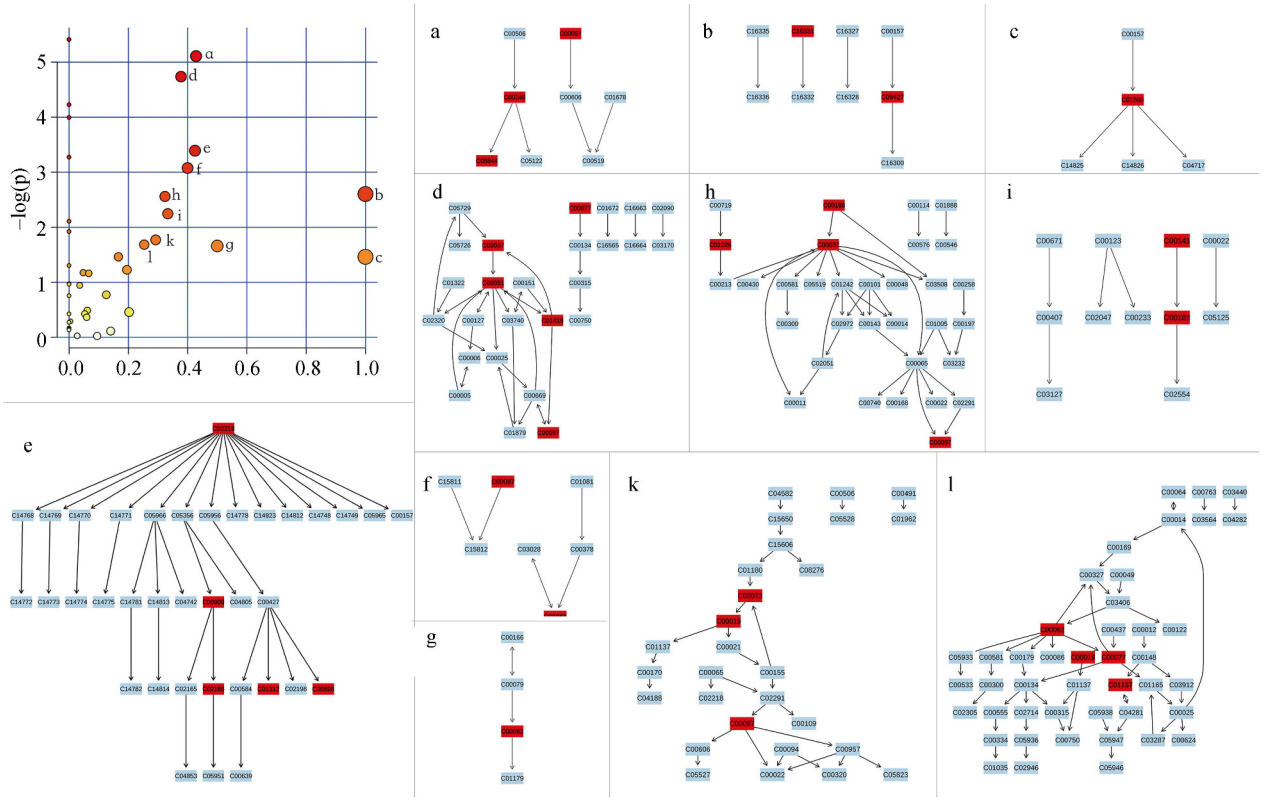

Fig. 7 Construction of the altered metabolism pathways in BD adjust the DBT using MetPA analysis. The map was generated using the reference map from KEGG; CO represents the entry number of the compounds: (a) taurine and hypotaurine metabolism; (b) alpha-linolenic acid metabolism; (c) linoleic acid metabolism; (d) glutathione metabolism; (e) arachidonic acid metabolism; (f) thiamine metabolism; (g) phenylalanine, tyrosine and tryptophan biosyntheses; (h) glycine, serine and threonine metabolism; (i) valine, leucine and isoleucine biosyntheses; (k) cysteine and methionine metabolism; and (l) arginine and proline metabolism. Red rectangles are entry selected different metabolites and KEGG IDs in the rectangles

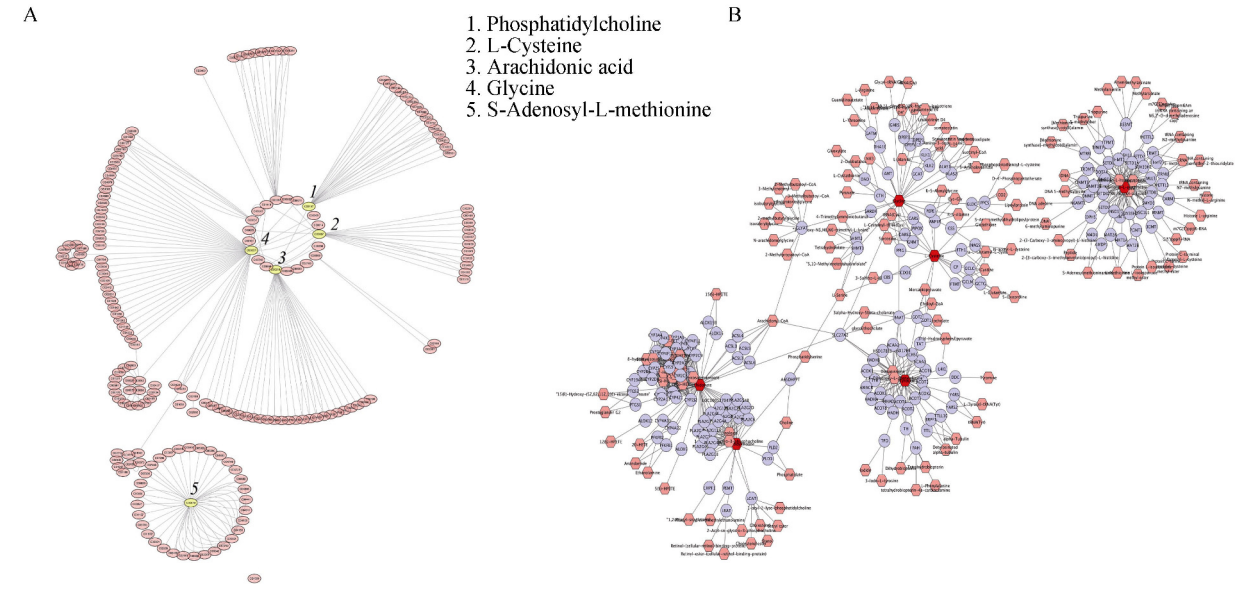

Fig. 8 (A) MetScape analysis of metabolite data; the hub metabolites with experimental data are shown in red. (B) Genes directly related to hub metabolite expression; hub metabolites with experimental data are shown in red and directly related genes are shown in lavender. Focal adhesion was identified as the most significant concept from the gene expression data by using LR path analysis

databases. The available pharmacological information—genomic and chemical—were used to predict the putative targets of the candidate compounds [12, 39]. A total of 167 putative targets were acquired for 44 of the 53 candidate compounds, the nine have not any related targets. Moreover, some different chemical compositions of DBT shared common or similar targets with therapeutic effects. To uncover the overall multi-target and multicomponent effects of the DBT-related herbs and to evaluate their mechanisms, a compounds-target network analysis was executed. We removed the nine compounds with no target proteins and a graph of compounds-target interactions was established (Fig. 9). The AR and AS of DBT possessed 167 putative targets that were the possible therapeutic targets (Fig. 9). A compound-target network was established for the 44 candidate compounds with their corresponding targets (detailed information about the compound–target network is provided in Table S10 of Supporting Information). Most of the active compounds were acted on more than one target. HQ18 obtained the highest number of targets (degree = 87), followed by HQ32 (degree = 67), HQ13 (degree = 60) and HQ7 (degree = 45). This result demonstrated these components have crucial roles. The average number of target proteins for AR and AS was 23. hence, the two herbs possessed multi-target properties. The average number of chemicals for every candidate target was 28, this result revealed the multicomponent features of the DBT. In these targets, PTGS2 obtained the largest degree (degree = 33), followed by PTGS1 (degree = 23), NCOA2 (degree = 21) and HSP90 (degree = 21). This finding demonstrated their potential therapeutic effects for treating anaemia.

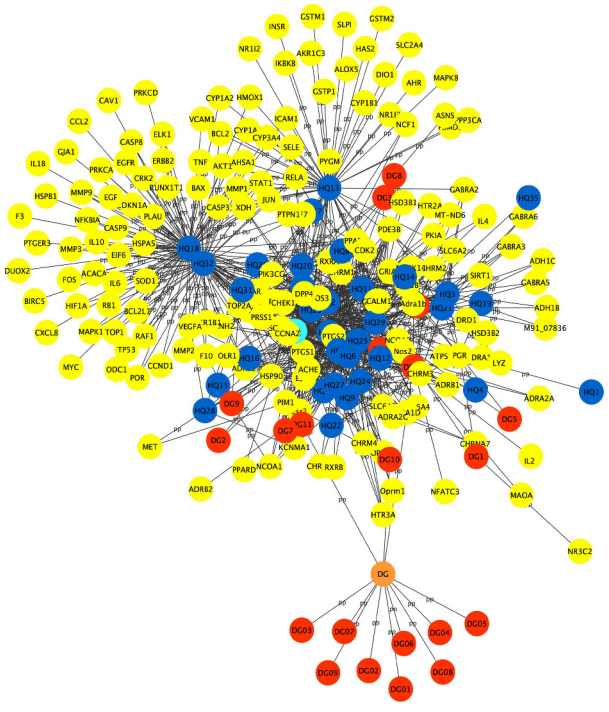

Fig.9 C–T network was constructed by linking the candidate compounds with their potential targets (yellow). DG, Radix Angelicae Sinensis(red); HQ, Radix Astragaliseu Hedysari(blue).

Identification of the candidate targets for DBT against anaemia

The systems biology study showed that anaemia proteins and genes are interlinked and exhibit PPI networks. To understand the role of various proteins in the anaemia [39], we established a target network of compound–putative in DBT (5959 nodes and 191 590 edges, Fig. 10A), an anaemia-related known target network (2294 nodes and 47 823 edges, Fig. 10B) and the target network of genes related the hub metabolites (3176 nodes and 66 462 edges, Fig. 10C). To reveal the pharmacological anti-anaemia mechanism of DBT, we included 7485 nodes and three networks with 162 095 edges. The reports showed that the degree of node is more than twice the median of all nodes and is an important target [36]. Therefore, we built an important target network of DBT with 1289 nodes and 56 145 edges (Fig. 10D). We chose six topological characteristics, namely, DC, BC, CC, EC, NC and LAC, to determine the candidate targets by using a plug-in called CytoNCA. The DC, LAC, CC, NC, EC and BC values were 89, 3, 100.812, 0.504, 0.0178, 18.09 and 15.13, respectively. A total of 288 candidate targets with the DC > 89, BC > 3, 100.812, CC > 0.504, EC > 0.0178, NC and LAC > 18.09 were selected for identification. The PPI networks and detailed topological features are represented in Fig. 10A–10F.

Enrichment analysis of the candidate targets for DBT against anaemia

ClueGO was used to determine the possible roles of the 288 candidate targets, discover the functional groups and identify the relationship and the basic scientific annotation of the biological networks [37]. According to the molecular function, biological processes, cell components and immune system processes, 288 candidate targets were classified into different categories (Fig. 11). The molecular function processes included iron ion binding, transferase activity, transferring a box, amino acid binding, oxidoreductase activity, acting on the matching donor (e.g. incorporation or reduction of molecular oxygen, reduced flavin or flavoprotein as one donor and incorporation of one oxygen atom), glutathione transferase activity and phospholipase A2 activity (Fig. 11A). The immune system processes were myeloid leukocyte mediated immunity, activation of the immune response, T cell activation and haemopoiesis (Fig. 11B). The biological processes were related to the organonitrogen compound metabolic process, small-molecule metabolic process, cellular lipid metabolic process, cellular amino acid metabolic process, P450 epoxygenase pathway, carboxylic acid catabolic process and so on (Fig. 11C). The cell component category included the peroxisomal part, mitochondrion, oxidoreductase complex, anchored component of membrane, endoplasmic reticulum membrane and MOZ/MPER histone acetyltransferase complex (Fig. 11D). Thus, the DBT can contributed to the blood enrichment effects on the APH- and CTX-induced BD rats by promoting the haematopoietic activities (by iron ion binding and haemopoiesis), inhibiting the production of reactive oxygen species (ROS) and inhibit the inflammation potentially.

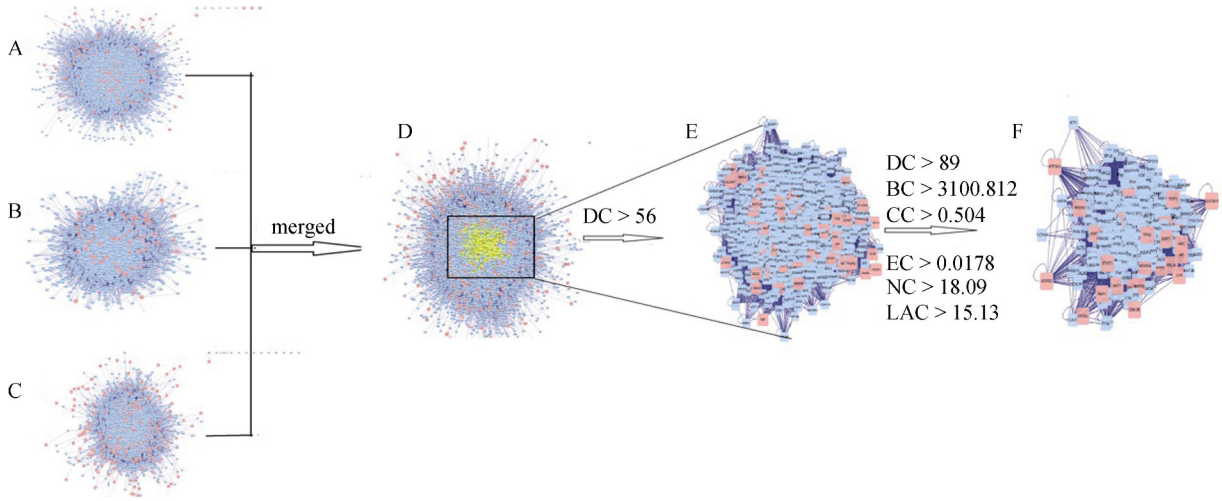

Fig. 10 (A) Compound-putative interactive PPI target network with 5959 nodes and 191 590 edges. (B) Anaemia-related target network with 2, 294 nodes and 47, 823 edges. (C) Target network of genes related to the hub metabolites with 3176 nodes and 66, 462 edges using the data. (D) The interaction PPI network of DBT putative targets and known BD-related targets with 4, 550 nodes and 128 542 edges. (E) PPI network of significant proteins extracted from with 1289 nodes and 56 145 edges. (F) PPI network of candidate DBT targets for BD treatment extracted from (E) with 288 nodes and 11 531 edges

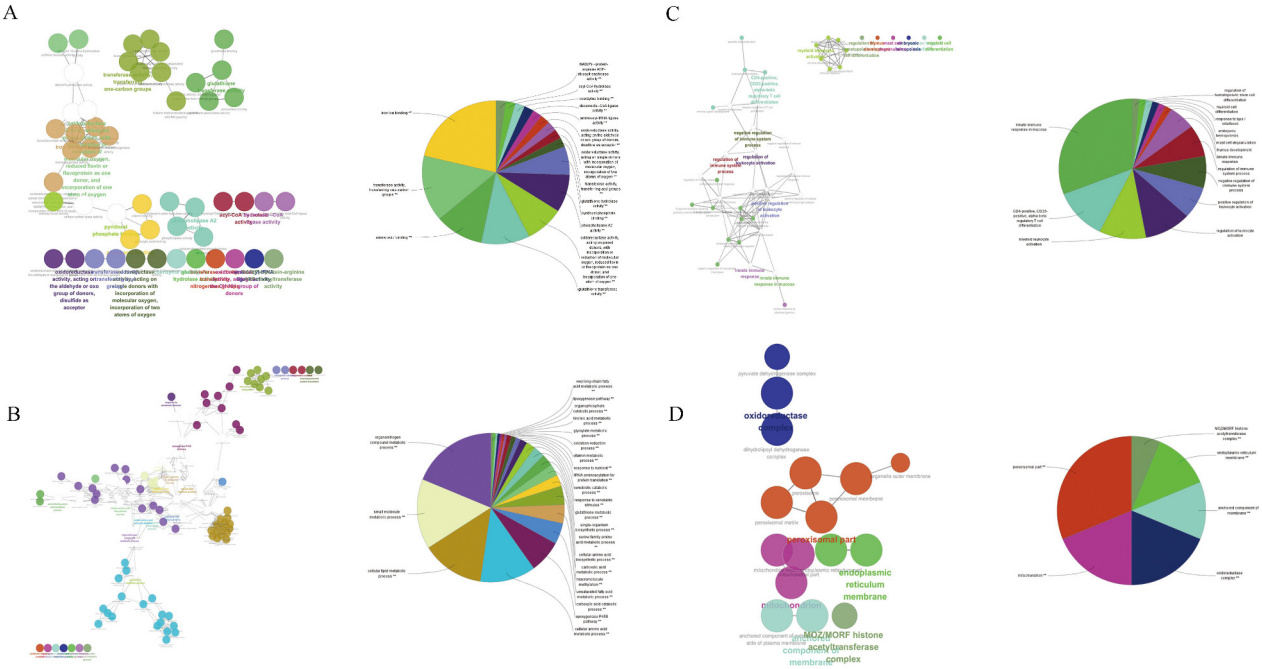

Fig. 11 ClueGO analysis of the predicted targets. Functionally grouped network of enriched categories was generated for the target genes. The GO terms represented the nodes, and the node size represented the term enrichment significance. Functionally related groups partially overlapped. The node pie charts represent the molecular function, immune system processes and reactome analysis of the targets. Only the most significant term in the group was labelled. Representative (A) Molecular Function, (B) Biological Processes, (C) Cell Component and (D) Immune System processes interactions among the targets

Discussion

A total of 44 potential compounds from the herbal constituents of DBT interacted with 167 putative targets, including PTGS2, PTGS1, HSP90, NCOA2, PRSS1, CHRM1, RXRA, PPARG, NOS2, DPP4, GABRA1, CALM1, nitric oxide synthase (NOS3), AR, ACHE, SCN5A, ESR2, ADRA1B, ESR1, ADRB2, CDK2, CHEK1, CHRM3, PDE3B, PGR, GSK3B, PIM1, TOP2A. Their index degrees were greater than or equal to 10. These proteins were related to the five hub metabolites (*S*-adenosyl-L-methionine, glycine, L-cysteine, AA and PC), their molecular functions processes were related to iron ion binding, transferase activity, transferring one box, amino acid binding, oxidoreductase activity, acting on paired

donors (incorporation or reduction of molecular oxygen, reduced flavin or flavoprotein as one donor and incorporation of one atom of oxygen), glutathione transferase activity, phospholipase A2 activity and so on. (Fig. 4A). The immune system processes were myeloid leukocyte mediated immunity, activation of the immune response, T cell activation and haemopoiesis (Fig. 10).

In the process of therapeutic targets of the predicted active compounds of DBT collection, combined keywords were used in TCMSP, ChemMapper, STITCH databases to cover a wider retrieval range avoiding missing targets. However, nine compounds have not any related targets can be found. In order to find out the underlying mechanism of DBT as far as possible, the targets list was manually checked one by one with references to avoid any missing. So, though nine compounds of DBT have not any related targets, the results were credibility and reliability and can used to analyze.

DBT enriched the blood by promoting haematopoietic activities

The function of iron ion binding is to interact selectively with iron ions. Iron is essential for most living organisms and plays an important role in the constituents of cytochromes, HGB, myoglobin and some enzymes [40-41]. In the current study, the inhibition assays revealed that cysteine proteases were involved in iron binding [42]. The active site of cysteine sulphide and 3-mercaptopropionic acid sulphate crystal show that the sulphide is through the combination of the distal sulphide. In the case of cysteine, the lead sulphide and amine combine [43]. In our study, the cysteine levels decreased in the BD rats. Cysteine was upregulated in BD by DBT. The systems pharmacology analysis (including the compound–putative targets, anaemia-related targets and hub metabolite gene-related networks) revealed that the iron ion binding was important in the enrichment of the blood pharmacological mechanisms of DBT on BD rat models. Iron ion binding possibly promoted haematopoiesis by increasing the heme-binding protein levels. The haematopoiesis was enriched as confirmed using ClueGo. Therefore, DBT was significantly involved in the haematopoietic effect. The haematopoietic activities possibly resulted from the stimulation of the iron ion transport, enhancement of bone marrow haematopoietic function and increase in cysteine level. However, some studies showed the interaction between metabolites changes and the gene expression profiles. Hence, whether the haematopoietic activities were caused by the increase of cysteine or of the heme-binding protein remains unclear.

DBT inhibited ROS production

Oxidoreductase activity binds the donor or the flavin or flavin protein as a donor to active oxygen by adding or reducing the molecular oxygen. The REDOX enzyme activity is a reversible catalytic REDOX reaction. In this kind of chemical reaction, the oxidation state of molecules or atoms change. A substrate is oxidised as a hydrogen or electron donor, whereas another is reduced as a hydrogen or electron acceptor.

In the present study, APH and CTX were used to establish the haemolytic and aplastic anaemia model [4, 24]. APH, a strong oxidant, exerts oxidative damage effects on RBCs resulting in haemolytic anaemia of the body [44] APH is a classic haemolytic drug and can produces hydrogen peroxide by a coupled oxidation with oxyhaemoglobin [45]. APH can deplete haematopoietic stem cells in the marrow and circulate peripheral blood cells resulting in anaemia (hematopoietic suppression) and immunodeficiency [4]. CTX is one of the most widely used chemotherapeutic agents [46] and can induce oxidative stress. Hence, ROS plays an important role in APH and CTX phases. However, excessive ROS generation can lead to changes in cell functions and eventually to cell death. PC, which was decreased in the BD group and upregulated in the plasma by DBT, is a phospholipid and is one of the key ingredients in the membrane. The formation of PC is responsible for all the important features of the membrane. The formation of oxidised phospholipid derivatives may lead to the increase of phospholipid polarity. Disorders in the phospholipid bilayer structure lead to the loss of structure and chemical properties of the membrane and even complete destruction of its integrity.

The oxidative activity of ants is affected by glycine, serine and threonine metabolism [47]. In the current study, the increase of glycine in the DB rats may be observed in the development of DBT. In plasma, the interference of antioxidant activity caused by DBT coincided with the metabolic biomarker (i.e. glycine). Our findings suggested a significant ROS reduction in the plasma of the treatment groups. Such decrease may be linked to glycine and the related enzyme, which have been shown to clear oxygen free radicals [48-49].

S-Adenosyl-methionine can reduce hepatic iron accumulation, oxidative stress and tissue injury in obstructed rats [50]. Metabolomics analysis showed that *S*-adenosyl-methionine was a hub metabolite for DBT in treating anaemia. The level of *S*-adenosyl-methionine increased in the DBT group compared with the anaemia group. Therefore, DBT interacted with the GSTP target, increased the levels of glycine and *S*-adenosyl-methionine and influenced the oxidoreductase activity, thus inhibiting ROS production.

DBT suppressed the inflammation in APH- and CTX-induced BD rats

Phospholipase A2 (PLA2) can stop, prevent or reduce its own activity. PLA2 catalyses the hydrolysis of phospholipid sn-2 ester bonds and facilitates phospholipid turnover leading to the release of polyunsaturated fatty acids (PUFAs) and pro-inflammatory lipid mediators [51–52]. PLA2 activation is the pivotal step in the effector pathway of inflammation [53]. The group IVA cytokinase A2 (GIVA cPLA2) is the main enzyme that causes the inflammatory AA to be released, with high specificity. In a receptor-mediated programme, the release of 15-hydroxyeicosatetraenoic acid from GIVA cPLA2 in primary and permanent biochemical macrophages is necessary for a complete inflammatory commitment [53]. AA can activate the inflammatory channel directly, and the opposite is

the same. In the preclinical model, it has an inflammatory signal (i.e. cytokines, which directly affects lipid metabolism) [54]. In our study, high AA concentrations were detected in the plasma of APH- and CTX-induced BD rats and were restored to the normal state after DBT administration. Linoleic acid metabolism and glycerolipid metabolism, alpha-linolenic acid metabolism and AA metabolism were filtered out as potential target pathways (Fig. 8), and AA was also selected as a hub metabolite (Fig. 9). These results were consistent with previous research results that volatile oils from *Angelica sinensis* exhibited good anti-inflammatory effects [55]. As shown in Fig. 8 and Table S3, multi-compounds interacted with two target proteins, including PTGS2 and PTGS1, which can be related to the AA release and inflammation.

In our results, NOS2 and NOS3 also were selected to be targets. NOS2-derived nitrogen oxides play an important role in inflammatory regulation [56], NOS3 may determine responsiveness to fatty acids [57], and fatty acids (PUFAs) play a critical role in the regulation of inflammatory signalling.

DBT involved in apoptosis regulation

Hsp90 were selected in our analysis which were related with the regulation of apoptosis. A previous study also showed that the expression of protein Hsp90 in CTX and APH induced anaemia model animals were increase and AS was a blockade of Hsp90 [58]. These results shown that DBT can prevent apoptosis during the anaemia process through upregulation HSP90.

In addition, PLA2 can sensitize a PLA2 receptor (PLA2R1) in the cell membrane. Despite the list of PLA2 targets to extends intracellular energy balance, glucose homeostasis, hepatic lipogenesis and adipocyte development, the PLA2R1 downstream effectors are few and scarcely investigated. Among the most addressed PLA2R1 effects are regulation of pro-inflammatory signalling, autoimmunity, apoptosis and senescence [59]. Apoptosis of rat sinusoidal endothelial cells which caused by deprivation of vascular endothelial cells can be prevented by glycine. Some results also revealed that the phospholipid metabolism enzyme PLA2 is an important regulator of apoptosis in several types of diseases. According this analysis, DBT can increase antiapoptosis.

Conclusion

A novel approach was utilised to evaluate the mechanism of DBT on APH- and CTX-induced anaemia based on a systems pharmacology analysis. *S*-adenosyl-L-methionine, glycine, L-cysteine, AA and PC were screened as hub metabolites. A total of 288 major candidate targets that were central to anaemia progression were identified for DBT. The gene-set enrichment analysis manifested that targets which we were selected were associated with iron ion binding, haemopoiesis, ROS production, apoptosis, inflammation and related signalling pathways.

In addition, it is not enough to conduct network pharmacological study only by MetScape analysis, compound–putative interactive PPI target network, ClueGO analysis, the multiple scale [60] and dynamic behaviors of the disease or drug network were also used in some researches [61-62]. In the future work, we will take into consideration the multiple scale and dynamic behaviors of the disease or drug network.

References

[1] Yang X, Huang CG, Du SY, *et al*. Effect of Danggui Buxue Tang on immune-mediated aplastic anemia bone marrow proliferation mice [J]. *Phytomedicine*, 2014, **21**(5): 640-646.

[2] Ning L, Jin RM, Wu YP, *et al*. Effect of components of danggui-bu-xue decoction on hematopenia [J]. *China J China Mater Med*, 2002, **27**(1): 50-53.

[3] Pang HQ, Tang YP, Cao YJ, *et al*. Comparatively evaluating the pharmacokinetic of fifteen constituents in normal and blood deficiency rats after oral administration of Xin-Sheng-Hua Granule by UPLC–MS/MS [J]. *J Chromatogr B*, 2017, **1061**: 372-381.

[4] Li W, Tang Y, Guo J, *et al*. Comparative metabolomics analysis on hematopoietic functions of herb pair Gui-Xiong by ultra-high-performance liquid chromatography coupled to quadrupole time-of-flight mass spectrometry and pattern recognition approach [J]. *J Chromatogr A*, 2014, **1346**: 49-56.

[5] Li PL, Sun HG, Hua YL, *et al*. Metabolomics study of hematopoietic function of *Angelica sinensis* on blood deficiency mice model [J]. *J Ethnopharmacol*, 2015, **166**: 261-269.

[6] Shi X, Tang Y, Zhu H, *et al*. Pharmacokinetic comparison of seven major bio-active components in normal and blood deficiency rats after oral administration of Danggui Buxue decoction by UPLC-TQ/MS [J]. *J Ethnopharmacol*, 2014, **153**(1): 169-177.

[7] Yang B, Liu Z, Wang Q, *et al*. Comparative tissue distribution profiles of five major bio-active components in normal and blood deficiency rats after oral administration of Danggui Buxue Decoction by UPLC-TQ/MS [J]. *J Pharm Biomed Anal*, 2017, **148**: 119.

[8] Zierau O, Zheng KYZ, Papke A, *et al*. Functions of Danggui Buxue Tang, a Chinese herbal decoction containing Astragali Radix and Angelicae Sinensis Radix, in uterus and liver are both estrogen receptor-dependent and -independent [J]. *Evid Based Complement Alternat Med*, 2014, **2014**: 1-11.

[9] Wang P, Liang YZ. Chemical composition and inhibitory effect on hepatic fibrosis of Danggui Buxue Decoction [J]. *Fitoterapia*, 2010, **81**(7): 793-798.

[10] Wang WL, Sheu SY, Chen YS, *et al*. Enhanced bone tissue regeneration by porous gelatin composites loaded with the Chinese herbal decoction Danggui Buxue Tang [J]. *PLoS One*, 2015, **10**(6): e0131999.

[11] Zhang Y, Bai M, Zhang B, *et al*. Uncovering pharmacological mechanisms of Wu-tou decoction acting on rheumatoid arthritis through systems approaches: drug-target prediction, network analysis and experimental validation [J]. *Sci Rep*, 2015, **5**: 9463.

[12] Li J, Zhao P, Li Y, *et al*. Systems pharmacology-based dissection of mechanisms of Chinese medicinal formula Bufei Yishen as an effective treatment for chronic obstructive pulmonary disease [J]. *Sci Rep*, 2015, **5**: 15290.

[13] Hopkins AL. Network pharmacology: the next paradigm in drug discovery [J]. *Nat Chem Biol*, 2008, **4**(11): 682-690.

[14] Park SY, Park JH, Kim HS, *et al*. Systems-level mechanisms of

action of *Panax ginseng*: a network pharmacological approach [J]. *J Gins Res*, 2018, **42**(1): 98-106.

[15] Yang M, Chen J, Xu L, *et al*. A network pharmacology approach to uncover the molecular mechanisms of herbal formula Ban-Xia-Xie-Xin-Tang [J]. *Evid Based Complement Alternat Med*, 2018, **2018**: 1-22.

[16] Yu G, Wang W, Wang X, *et al*. Network pharmacology-based strategy to investigate pharmacological mechanisms of Zuojinwan for treatment of gastritis [J]. *BMC Complement Altern Med,* 2018, **18**(1): 292.

[17] Chen L, Cao Y, Zhang H, *et al*. Network pharmacology-based strategy for predicting active ingredients and potential targets of Yangxinshi tablet for treating heart failure [J]. *J Ethnopharmacol*, 2018, **219**: 359-368.

[18] Cui Y, Li C, Zeng C, *et al*.Tongmai Yangxin pills anti-oxidative stress alleviates cisplatin-induced cardiotoxicity: Network pharmacology analysis and experimental evidence [J]. *Biomed Pharmacother*, 2018, **108**: 1081-1089.

[19] Zhao S, Liu Z, Wang M, *et al*. Anti-inflammatory effects of Zhishi and Zhiqiao revealed by network pharmacology integrated with molecular mechanism and metabolomics studies [J]. *Phytomedicine*, 2018, **50**: 61-72.

[20] Xiang Z, Sun H, Cai X, *et al*. The study on the material basis and the mechanism for anti-renal interstitial fibrosis efficacy of rhubarb through integration of metabonomics and network pharmacology [J]. *Mol BioSyst*, 2015, **11**(4): 1067-1078.

[21] Liu J, Mu J, Zheng C, *et al*. Systems-pharmacology dissection of traditional chinese medicine compound saffron formula reveals multi-scale treatment strategy for cardiovascular diseases [J]. *Sci Rep*, 2016, **6**: 19809.

[22] Kell DB, Goodacre R. Metabolomics and systems pharmacology: why and how to model the human metabolic network for drug discovery [J]. *Drug Discov Today*, 2014, **19**(2): 171-182.

[23] Gong AG, Li N, Lau KM, *et al*. Calycosin orchestrates the functions of Danggui Buxue Tang, a Chinese herbal decoction composing of Astragali Radix and Angelica Sinensis Radix: An evaluation by using calycosin-knock out herbal extract [J]. *J Ethnopharmacol*, 2015, **168**: 150-157.

[24] Jia L, Yu J, He L, *et al*. Nutritional support in the treatment of aplastic anemia [J]. *Nutrition*, 2011, **27**(11-12): 1194-1201.

[25] Smith CA, Want EJ, O'Maille G, *et al*. XCMS: Processing mass spectrometry data for metabolite profiling using nonlinear peak alignment, matching, and identification [J]. *Anal Chem*, 2006, **78**(3): 779-787.

[26] Wang L, Hou E, Wang L, *et al*. Reconstruction and analysis of correlation networks based on GC-MS metabolomics data for young hypertensive men [J] *Anal Chim Acta*, 2015, **854**: 95-105.

[27] Martin A, Ochagavia ME, Rabasa LC, *et al*. BisoGenet: a new tool for gene network building, visualization and analysis [J]. *BMC Bioinformatics*, 2010, **11**(1): 91.

[28] Li Y, Zhang J, Zhang L, *et al*. Systems pharmacology to decipher the combinational anti-migraine effects of Tianshu formula [J]. *J Ethnopharmacol*, 2015, **174**: 45-56.

[29] Wang J, Li Y, Yang Y, *et al*. Systems pharmacology dissection of multiscale mechanisms of action for herbal medicines in treating rheumatoid arthritis [J]. *Mol Pharm*, 2017, **14**(9): 3201-3217.

[30] Liu H, Wang J, Zhou W, *et al*. Systems approaches and polypharmacology for drug discovery from herbal medicines: an example using licorice [J]. *J Ethnopharmacol*, 2013, **146**(3): 773-793.

[31] Xu X, Zhang W, Huang C, *et al*. A novel chemometric method for the prediction of human oral bioavailability [J]. *Int J Mol Sci*, 2012, **13**(12): 6964-6982.

[32] Wishart DS, Knox C, Guo AC, *et al*. DrugBank: a knowledgebase for drugs, drug actions and drug targets [J]. *Nucleic Acids Res*, 2008, **36**(Database issue): 901-906.

[33] Hamosh A, Scott AF, Amberger JS, *et al*. Online Mendelian Inheritance in Man (OMIM), a knowledgebase of human genes and genetic disorders [J]. *Nucleic Acids Res*, 2005, **33**(1): 514-517.

[34] Becker KG, Barnes KC, Bright TJ, *et al*. The genetic association database [J]. *Nat Genet*, 2004, **36**(5): 431-432.

[35] Doerks T, Copley RR, Schultz J, *et al*. Cytoscape: a software environment for integrated models of biomolecular interaction networks [J]. *Genome Res*, 2003, **13**: 2498-2504.

[36] Tang Y, Li M, Wang J, *et al*. CytoNCA: a cytoscape plugin for centrality analysis and evaluation of protein interaction networks [J]. *Biosystems*, 2015, **127**: 67-72.

[37] Bindea G, Mlecnik B, Hackl H, *et al*. ClueGO: a Cytoscape plug-in to decipher functionally grouped gene ontology and pathway annotation networks [J]. *Bioinformatics*, 2009, **25**(8): 1091-1093.

[38] Liu YF, Ai N, Fan XH, *et al*. Network pharmacology for traditional Chinese medicine research: methodologies and applications [J]. *Chin Herb Med*, 2015, **7**(1): 18-26.

[39] Yu H, Chen J, Xu X, *et al*. A systematic prediction of multiple drug-target interactions from chemical, genomic, and pharmacological data [J]. *PLoS One*, 2012, **7**(5): e37608

[40] Zumbrennenbullough K, Babitt JL. The iron cycle in chronic kidney disease (CKD): from genetics and experimental models to CKD patients [J]. *Nephrol Dial Transplant*, 2014, **29**(2): 263.

[41] Huang CY, Wu CH, Yang JI, *et al*. Evaluation of iron-binding activity of collagen peptides prepared from the scales of four cultivated fishes in Taiwan [J]. *J Food Drug Anal*, 2015, **23**(4): 671-678.

[42] Moisés MC, Gerardo RR, Jesús SL, *et al*. Iron-binding protein degradation by cysteine proteases of Naegleria fowleri [J]. *Biomed Res Int*, 2015, **2015**: 1-8.

[43] Souness RJ, Kleffmann T, Tchesnokov EP, *et al*. Mechanistic implications of persulfenate and persulfide binding in the active site of cysteine dioxygenase [J]. *Biochemistry*, 2013, **52**(43): 7606-7617.

[44] Croci S, Pedrazzi G, Passeri G, *et al*. Acetylphenylhydrazine induced haemoglobin oxidation in erythrocytes studied by Mossbauer spectroscopy [J]. *Biochim Biophys Acta*, 2001, **1568**(1): 99-104.

[45] Liebowitz J, Cohen G. Increased hydrogen peroxide levels in glucose 6-phosphate dehydrogenase deficient erythrocytes exposed to acetylphenylhydrazine [J]. *Biochem Pharmacol*, 1968, **17**(6): 983-988.

[46] Xu M, He RR, Zhai YJ, *et al*. Effects of carnosine on cyclophosphamide-induced hematopoietic suppression in mice [J]. *Am J Chin Med,* 2014, **42**(1): 131-142.

[47] Amelio I, Cutruzzolá, F, Antonov A, *et al*. Serine and glycine metabolism in cancer [J]. *Trends Biochem Sci*, 2014, **39**(4): 191-198.

[48] Lin HQ, Gong AGW, Wang HY, *et al*. Danggui Buxue Tang (Astragali Radix and Angelicae Sinensis Radix) for menopausal symptoms: A review [J]. *J Ethnopharmacol*, 2017, **199**: 205-210.

[49] Wang LY, Tang YP, Liu X, *et al*. Effects of ferulic acid on antioxidant activity in Angelicae Sinensis Radix, Chuanxiong Rhizoma, and their combination [J]. *Chin J Nat Med*, 2015, **13**(6): 401-408.

[50] Munoz-Castaneda JR, Tunez I, Herencia C, *et al*. Melatonin exerts a more potent effect than S-adenosyl-l-methionine against iron metabolism disturbances, oxidative stress and tissue injury induced by obstructive jaundice in rat [J]. *Chem Biol Interact*, 2008, **174**(2): 79-87.

[51] Pruzanski W, Vadas P. Phospholipase A2 and inflammation [J]. *Ann Rheum Dis*, 1989, **48**(11): 962-963.

[52] Hanasaki K, Arita H. Biological and Pathological Functions of Phospholipase A2 Receptor [J]. *Arch Biochem Biophys*, 1999, **372**(2): 215-223.

[53] Norris PC, Gosselin D, Reichart D, *et al*. Phospholipase A2 regulates eicosanoid class switching during inflammasome activation [J]. *Proc Natl Acad Sci*, 2014, **111**(35):12746-12751.

[54] Van Diepen JA, Berbée Jimmy FP, Havekes LM, *et al*. Interactions between inflammation and lipid metabolism: Relevance for efficacy of anti-inflammatory drugs in the treatment of atherosclerosis [J]. *Atherosclerosis*, 2013, **228**(2): 306-315.

[55] Hua YL, Ji P, Xue ZY, *et al*. Construction and analysis of correlation networks based on gas chromatography-mass spectrometry metabonomics data for lipopolysaccharide-induced inflammation and intervention with volatile oil from Angelica sinensis in ratsConstruction and analysis of correlation networks based on gas chromatography-mass spectrometry metabonomics data for lipopolysaccharide-induced inflammation and intervention with volatile oil from Angelica sinensis in rats [J]. *Mol Biosyst*, 2015, **11**(11): 3174-87.

[56] Guo C, Atochina-Vasserman E, Abramova H, *et al*. Role of NOS2 in pulmonary injury and repair in response to bleomycin [J]. *Free Radic Biol Med*, 2016, **91**: 293-301.

[57] Ferguson JF, Phillips CM, Mcmonagle J, *et al*. NOS3 gene polymorphisms are associated with risk markers of cardiovascular disease, and interact with omega-3 polyunsaturated fatty acids [J]. *Atherosclerosis*, 2010, **211**(2): 539-544.

[58] Hua Y, Yao W, Ji P, *et al*. Integrated metabonomic-proteomic studies on blood enrichment effects of Angelica sinensis on a blood deficiency mice model [J]. *Pharm Biol*, 2017, **55**(1): 853-863.

[59] Sukocheva O, Menschikowski M, Hagelgans A, *et al*. Current insights into functions of phospholipase A2 receptor in normal and cancer cells: More questions than answers [J]. *Semin Cancer Biol*, 2017, **2**(17): 30180-30183.

[60] Guo Y, Nie Q, Maclean AL, *et al*. Multiscale modeling of inflammation-induced tumorigenesis reveals competing oncogenic and oncoprotective roles for inflammation [J]. *Cancer Res*, 2017, **77**(22): 6429-6441.

[61] Li S, Zhang B. Traditional Chinese medicine network pharmacology: theory, methodology and application [J]. *Chin J Nat Med*, 2013, **11**(2): 11.

[62] Liang X, Li H, Li S. A novel network pharmacology approach to analyse traditional herbal formulae: the Liu-Wei-Di-Huang pill as a case study [J]. *Mol Biosyst*, 2014, **10**(5): 1014.

Cite this article as: HUA Yong-Li, MA Qi, YUAN Zi-Wen, ZHANG Xiao-Song, YAO Wan-Ling, JI Peng, HU Jun-Jie, WEI Yan-Ming. A novel approach based on metabolomics coupled with network pharmacology to explain the effect mechanisms of Danggui Buxue Tang in anaemia [J]. *Chin J Nat Med*, 2019, **17**(4): 275-290.